



INSTITUT DE FRANCE
Académie des sciences

Comptes Rendus

Géoscience

Sciences de la Planète

Pierangelo Romano, Ida Di Carlo, Joan Andújar and Silvio G. Rotolo

Water solubility in trachytic and pantelleritic melts: an experimental study


Online first, 8th September 2021

<<https://doi.org/10.5802/crgeos.75>>

Part of the Special Issue: Perspectives on alkaline magmas

Guest editor: Bruno Scaillet (Institut des Sciences de la Terre d'Orléans, CNRS, France)

© Académie des sciences, Paris and the authors, 2021.
Some rights reserved.

 This article is licensed under the
CREATIVE COMMONS ATTRIBUTION 4.0 INTERNATIONAL LICENSE.
<http://creativecommons.org/licenses/by/4.0/>



*Les Comptes Rendus. Géoscience — Sciences de la Planète sont membres du
Centre Mersenne pour l'édition scientifique ouverte*
www.centre-mersenne.org



Perspectives on alkaline magmas / *Perspectives sur les magmas alcalins*

Water solubility in trachytic and pantelleritic melts: an experimental study

Pierangelo Romano[✉]*, a, b, Ida Di Carlo^c, Joan Andújar^c and Silvio G. Rotolo^{a, b}

^a Istituto Nazionale di Geofisica e Vulcanologia, sezione di Palermo, Via Ugo la Malfa 153, 90146 Palermo, Italy

^b Dipartimento di Scienze della Terra e del Mare (DiSTeM), Università degli Studi di Palermo, Via Archirafi 22, 90123 Palermo, Italy

^c Institut des Sciences de la Terre d'Orléans (ISTO) UMR 7327, Université d'Orléans – CNRS – BRGM, Campus Géosciences, 1A rue de la Férellerie, 45071 Orleans Cedex 2, France

E-mails: pierangeloromano@gmail.com (P. Romano), ida.di-carlo@cnrs-orleans.fr (I. Di Carlo), juan.andujar@cnrs-orleans.fr (J. Andújar), silvio.rotolo@unipa.it (S. G. Rotolo)

Abstract. Solubility experiments were performed on a trachyte and a pantellerite from Pantelleria. The trachyte has $\text{SiO}_2 = 65.2$ wt%, $\text{Al}_2\text{O}_3 = 15.2$ wt% and a peralkaline index (P.I. = molar[($\text{Na}_2\text{O} + \text{K}_2\text{O}$)/ Al_2O_3]) ~ 1 while the pantellerite has $\text{SiO}_2 = 72.2$ wt%, $\text{Al}_2\text{O}_3 = 11$ wt% and a P.I. = 1.3. Solubility experiments were performed in the pressure range of 50–300 MPa at $T = 950$ °C for the trachyte and 50–200 MPa at $T = 850$ °C for the pantellerite. The water content of experimental glasses was determined by Karl Fischer titration, elemental analyser and FT-IR spectroscopy. Water content appears similar in both compositions for analogous pressure conditions, varying from ~ 2.5 wt% at 50 MPa to ~ 5.8 at 200 MPa. Comparison of the experimental data with the thermodynamic models shows that the empirical model of Moore et al. [1998] better matches the experimental data for both compositions, while the thermodynamic models of Papale et al. [2006] and Giorso and Gualda [2015] tend to overestimate melt water content, probably due to the paucity of peralkaline melt compositions used for calibration. One inference of these new solubility data is on MI-derived depth of felsic reservoirs at Pantelleria which deepens from 2.4 to 3.5 km.

Keywords. Trachyte, Pantellerite, Water solubility, Experiments, Alkaline magmas.

Online first, 8th September 2021

1. Introduction

Water solubility in silicate melts has been widely investigated because of the important effects it has on magma properties, such as viscosity and density [e.g. Dingwell et al., 1996, Richet et al.,

1996], liquidus and solidus temperatures, phase compositions [e.g. Sisson and Grove, 1993] and mineral stabilities [Housh and Luhr, 1991, Holtz et al., 1992], and crystallization kinetics [e.g. Watson, 1994, Cashman and Mangan, 1994, Arzilli et al., 2020] and eruptive dynamics [e.g. Cassidy et al., 2018]. Water solubility has been thoroughly investigated in basaltic and rhyolitic compositions [e.g. Hamilton et al., 1964, Silver et al., 1990, Dixon et al., 1995,

* Corresponding author.

Moore *et al.*, 1998, Behrens and Jantos, 2001, Tamic *et al.*, 2001, Liu *et al.*, 2005, Lesne *et al.*, 2010] for which the general effects of composition, particularly that of alkalis and silica contents [e.g. Johannes and Holtz, 1996, Romano *et al.*, 1996, Dingwell *et al.*, 1997, Holtz *et al.*, 2000, Behrens *et al.*, 2001, Schmidt and Behrens, 2008, Stabile *et al.*, 2018, 2020], and pressure–temperature are well established [e.g. Holtz *et al.*, 1992, 1995, Behrens *et al.*, 2001]. More recently, several studies have also focused their attention on intermediate compositions such as andesite–dacite [Mandeville *et al.*, 2002, Botcharnikov *et al.*, 2006, Behrens *et al.*, 2004], phonotephrite [Behrens *et al.*, 2009] and phonolite [Carroll and Blank, 1997, Larsen and Gardner, 2004, Iacono-Marziano *et al.*, 2007, Schmidt and Behrens, 2008] melts. In contrast, less attention has been paid to compositions such as trachytic melts, which usually represents the parental composition to peralkaline rhyolite/phonolite melts: only Di Matteo *et al.* [2004] and Fanara *et al.* [2015] have obtained solubility data on such compositions. Trachyte and pantellerite magmas are involved in explosive eruptions, some of which can be of large magnitude (e.g. Tambora 1815, Campanian Ignimbrite 39 kyr, Green Tuff 45 kyr), and it is therefore vital to accurately constrain water solubility in such melts. Enlarging the spectrum of available solubility data is also crucial to further improve already existing solubility models [e.g. Papale *et al.*, 2006, Ghiorsio and Gualda, 2015].

Here, we present new experimental H₂O solubility data obtained on trachytic and pantelleritic melts over the pressure range of 50–300 MPa. The trachyte and pantellerite used in this study are representative of the most abundant magmas on Pantelleria island. The water contents dissolved in experimental glasses have been determined by FT–IR spectroscopy, Karl Fischer titration (KFT) and elemental analyser (EA). The necessity of performing additional experiments arises from the observed dependence of water solubility on the composition of silicate melts, as several studies quoted above have illustrated. In particular, a small variation in melt chemical composition influences not only water solubility but also the extrapolation of molar absorption coefficients. FT–IR spectroscopy is a common tool used to determine the water content of natural volcanic products (melt inclusions and glassy groundmasses) but its accuracy is strongly related to the use of proper absorp-

tion coefficients, calibrated on compositions similar to that of natural glasses investigated. Otherwise, the extrapolation of absorption coefficients outside the calibration range may lead to a significant error in water determination. For this reason, in this work, we also used the results of FT–IR spectroscopy, KFT and EA analyses to determine the IR molar absorption coefficients for 4500 and 5200 cm⁻¹ bands by using the peak intensity and a straight line correction procedure [Stabile *et al.*, 2020, and reference therein].

2. Starting material and experimental strategy

2.1. Starting material and charges preparation

We used, as starting materials, natural samples representative of the trachytic and peralkaline rhyolite (pantellerite) of Pantelleria Island (Table 1). Pantelleria, located in the Sicily Channel, is the type locality for pantellerite, an iron-rich rhyolite characterized by alkali/alumina molar ratio $[(\text{Na}_2\text{O} + \text{K}_2\text{O})/\text{Al}_2\text{O}_3] > 1$ [Macdonald, 1974]. Pantellerites and trachytes are the most abundant rocks outcropping in the island and also in other localities, usually representing the felsic end member in continental rift zones (Pantelleria, Ethiopian Rift valley, etc.) or in oceanic islands (Mayor Island, Azores, etc.). The trachyte (sample GTT) and pantellerite (sample Pan113) specimen used in this study have been the subject of phase equilibrium experiments by Di Carlo *et al.* [2010] and Romano *et al.* [2018, 2020]. To prepare the starting materials, the selected rocks were finely crushed and the resulting powders were melted twice at 1300 °C for 3 h, then rapidly quenched. The glasses obtained were grinded in an agate mortar obtaining a powder of 10–40 μm mesh size. This technique, used in several previous experimental works [Di Carlo *et al.*, 2010, Romano *et al.*, 2020], allows to produce a crystal-free and homogeneous glass with a composition similar to the starting bulk rock. Experimental charges were prepared by loading 50–100 mg of dry glass powder and 5–10 mg distilled water in gold capsules, ensuring volatile saturation at experimental conditions. At 50 MPa, the amount of water loaded was slightly lower, to avoid the risk of capsule rupture. Once prepared, capsules were weighed and welded, then weighed again to verify any water loss during welding. Gold capsules were preferred to platinum or gold–palladium containers in order to minimize iron loss to the capsule walls, since the duration

Table 1. Chemical composition of experimental glasses

	<i>T</i> (°C)	<i>P</i> (MPa)	SiO ₂	TiO ₂	Al ₂ O ₃	FeO	MnO	MgO	CaO	Na ₂ O	K ₂ O	P ₂ O ₅	Total	Original total	PI.
Green Tuff Trachyte (GTT)															
Starting material			64.12	0.85	15.04	6.27	0.27	0.62	1.48	6.58	4.6	0.17	100		1.05
GT R11-1	950	50	65.27	0.87	15.07	5.32	0.19	0.63	1.45	6.74	4.7	0.21	100	94.82	1.07
sd			0.62	0.07	0.32	0.31	0.08	0.04	0.06	0.26	0.09	0.09		0.98	
GT R10-1	950	100	65.62	0.77	15.46	4.79	0.24	0.6	1.33	6.33	4.65	0.21	100	95.57	1.00
sd			0.55	0.08	0.17	0.25	0.09	0.03	0.05	0.73	0.16	0.07		0.89	
GT R 9-1	950	150	65.23	0.95	15.24	5.34	0.35	0.65	1.54	6.46	4.55	0.29	100	94.51	1.02
sd			0.36	0.07	0.11	0.23	0.07	0.03	0.04	0.81	0.18	0.09		0.94	
GT R 15-1	985	200	65.60	0.88	14.86	5.58	0.22	0.62	1.50	6.17	4.37	0.20	100	95.59	1.00
sd			0.36	0.10	0.18	0.26	0.12	0.03	0.06	0.62	0.14	0.09		0.67	
GT R 18-2	985	200	65.14	0.86	15.00	5.56	0.20	0.63	1.48	6.51	4.43	0.20	100	95.59	1.03
sd			0.46	0.09	0.22	0.19	0.09	0.03	0.05	0.56	0.14	0.08		0.73	
GT R19-1	985	300	65.06	0.80	15.04	5.25	0.23	0.61	1.42	7.14	4.28	0.18	100	91.76	1.09
sd			0.33	0.11	0.15	0.29	0.11	0.03	0.04	0.35	0.11	0.09		0.57	
GT R16-1	985	300	65.28	0.87	15.55	5.64	0.21	0.60	1.50	5.39	4.57	0.39	100	90.84	0.89
sd			0.74	0.09	0.65	0.26	0.10	0.03	0.05	0.20	0.16	0.12		0.50	
Pantellerite (Pan113)															
Starting Material			69.45	0.48	10.15	7.87	0.21	0.10	0.53	6.71	4.46	0.04	100		1.56
Run C-Run L	850	50	72.64	0.37	10.90	5.28	0.32	0.19	0.35	5.02	4.94		100	93.49	1.25
sd			0.96	0.11	0.33	0.56	0.16	0.21	0.38	0.21	0.17			0.69	
Run A-RunH	850	100	72.56	0.44	11.20	4.85	0.23	0.22	0.37	5.12	5.00		100	91.89	1.24
sd			0.47	0.07	0.14	0.27	0.14	0.03	0.03	0.58	0.19			0.38	
Run B2	850	150	72.83	0.36	11.61	4.40	0.30	0.15	0.23	5.03	5.09		100	90.06	1.19
sd			0.14	0.06	0.13	0.16	0.10	0.04	0.05	0.21	0.17			0.56	
Run F	850	200	70.91	0.42	10.35	7.58	0.29	0.08	0.51	5.16	4.61		100	89.25	1.30
sd			0.31	0.06	0.15	0.23	0.13	0.01	0.09	0.10	0.13			0.76	

sd: standard deviation; PI.: peralkalinity index.

of the experiments exceeded the 24 h. The applied temperature was higher than 950 °C for trachytes and 850 °C for pantellerites, conditions that in both cases ensured to be above the liquidus in our experimental runs [Di Carlo *et al.*, 2010, Romano *et al.*, 2018, 2020]. Prior to experiments, capsules were left at least for 24 h in an oven at 120 °C to allow the homogenisation of water throughout the capsule.

2.2. Experimental strategy

Experiments were performed in internally heated pressure vessels (at Institut des Sciences de la Terre d'Orléans) equipped with a molybdenum furnace and a fast quench device. As pressurizing medium, a mixture of argon and hydrogen loaded in the vessel at room temperature was used: the Ar/H₂ ratio was fixed to reach redox condition around the FMQ buffer [e.g. Scaillet *et al.*, 1992, 1995, Romano *et al.*, 2020]. The pressure was recorded by a transducer calibrated against an Heise-Bourdon tube gauge (uncertainty ± 20 bar) while the temperature

was continuously controlled through S-type thermocouples (accuracy ± 5 °C). Experiments were performed in a *T* range 950–985 °C for trachytes and at 850 °C for pantellerites. The pressure range explored varied from 50 to 300 MPa (at 50 MPa intervals) and the duration of each experiment was between 96 and 125 h. Experiments were terminated using the drop-quench technique, which ensures a fast quench of the capsules from the top to the bottom of the vessel (quench rate >100 °C·s⁻¹). After the experiments, capsules were weighed to check for leaks and if the post run weight difference was >0.4 mg, capsules were discarded. The excess of H₂O within the capsule was confirmed by the occurrence of small water drops during the opening of the capsules, establishing that saturation conditions were reached during the experiment. For each capsule, around one-third of the run product was embedded in epoxy resin for qualitative analysis by a scanning electron microscope (SEM-EDS) and chemical analysis by an electron microprobe (EMP) while the remaining part was used to determine water contents.

3. Analytical methods

3.1. Scanning electron microscope and electron microprobe analyses

Glass fragments mounted in epoxy resin were first observed with a SEM and then analysed by an EMP to check glass for composition and homogeneity. EMP analyses were performed with a Cameca SX-Five located at CNRS-ISTO laboratory (France). Analytical conditions were an accelerating voltage of 15 kV, a beam current of 6 nA and a defocused beam of $10 \times 10 \mu\text{m}$. Na and K were analysed first to minimize volatile loss during the analyses. Microprobe analyses of alkali-rich hydrous glasses in some cases resulted problematic due to the alkali (mostly sodium) migration out of the excited volume. As suggested by Morgan and London [2005], we have used a current density of $0.006 \text{ nA}/\mu\text{m}^2$ that limits the Na migration under the beam and also provides adequate excitation of all elements.

3.2. Karl Fischer titration and elemental analyser

The total water contents of experimental glasses were determined by KFT and EA (EA Thermo Scientific Flash 2000) both housed at CNRS-ISTO laboratory. In KFT analysis, 10–20 mg of glass fragments are placed within a Pt crucible in an induction furnace and heated up to 1300 °C. Water liberated during the heating of glass fragments reacts quantitatively in a titration cell with iodine. The EA allows determining the concentration of H–C–N in experimental samples. In our case, only H₂ was measured to infer water content. The glass in the EA is first heated to 1800 °C upon which the substance oxidizes into simple compounds, which are in turn quantified by thermal conductivity detection. Moussallam *et al.* [2015] used this technique to determine water and CO₂ contents in kimberlite melts. The EA was calibrated before each analytical session using pure pyrophyllite, which is known to contain 5 wt% of stoichiometric H₂O in its crystalline structure. The experimental samples for the EA were prepared by grinding 1–10 mg of experimental glass into a fine powder and then loading it in a tin capsule folder. The instrument was tested repeatedly using an international standard with known amounts of carbon, hydrogen and

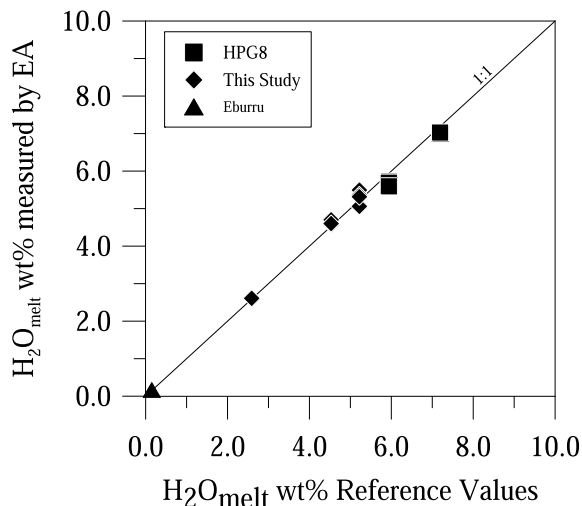


Figure 1. Comparison between water content in silica-rich melts analysed by EA and KFT; analyses on experimental glasses synthesized in this study, haplogranite (HPG8) composition [Dingwell *et al.*, 1997] and Eburru obsidian [Scaillet and Macdonald, 2006].

nitrogen and also using other hydrated glass samples (as internal standards) prepared for this purpose and for which water concentration was already known (haplogranite) or already analysed with KFT. In Figure 1 (Table 2), the water content determined by EA is compared with literature data for haplogranite composition [Dingwell *et al.*, 1997], Eburru obsidian [Scaillet and Macdonald, 2006] and KFT analyses of this study; a good correlation is observed between H₂O contents retrieved by these different techniques.

3.3. Density determination

Densities of anhydrous trachytic and pantelleritic starting glasses were measured by weighing single pieces of glass in air and ethanol. The determination of hydrous glass densities was more difficult because of the limited amount of run products; a minimum weight of 15 mg is indeed required to perform an accurate Archimedean density measure. Only for three hydrous trachytic glasses were reliable density data obtained (Figure 2a, Table 3), which was used to derive an empirical relationship of the form $\rho = -4.4017(\text{H}_2\text{O}_{\text{melt}} \text{ wt}\%) + 2329$. Standard deviation for

Table 2. Comparison of water content measured by Elemental Analyser and reference value

	Experimental pressure (MPa)	Elemental analyser	Reference values*
HPG8 GT R18-5	200	5.72	5.94
HPG8 GT R18-5	200	5.69	5.94
HPG8 GT R18-5	200	5.59	5.94
HPG8 GT R19-4	300	6.99	7.19
HPG8 GT R19-4	300	6.99	7.19
HPG8 GT R19-4	300	7.03	7.19
Pan 113 RUNB-1	150	5.06	5.22
Pan 113 RUNB	150	5.49	5.22
Pan 113 RUNB-2	150	5.36	5.22
Pan 113 RUN B	150	5.32	5.22
Pan 113 RUN C	50	2.61	2.59
Pan 113 RUNH	100	4.70	4.53
Pan 113 RUNH	100	4.57	4.53
Pan 113 RUNH	100	4.60	4.53
Eburru natural sample		0.17	0.15

* Reference value for HPG8 are from Dingwell *et al.* [1997].

Pan 113 and Eburru natural sample were analysed by Karl Fischer titration.

density values was estimated from repeated measures of glass fragments. For comparison, the densities of hydrous experimental glasses were also calculated using the procedure of Ochs and Lange [1999], calculated values being 4 to 11% higher than those measured. A less clear relationship has been found between density and melt water content for pantelleritic experimental glasses (Figure 2b, Table 3) and calculated densities are 1 to 6% higher relative to measured ones. To maintain internal consistency, we preferred to use the density measured or calculated from the above empirical relationship, knowing that density measurements are affected by relative errors in the range 0.1–2.5%.

3.4. FT-IR spectroscopy

Fourier Transform Infrared analyses were performed using a Nicolet 760 Magna spectrometer connected to an IR microscope (fluxed with H₂O-free compressed air) housed at ISTO laboratory. The spectrometer was equipped with an MCT detector, a Globar light source and a KBr beam splitter. Absorption spectra were acquired for each sample in the range 1000–6000 cm⁻¹ with 128 scans and a resolution of 4 cm⁻¹. Experimental glass chip samples were placed on an NaCl crystal plate, which is transparent

to the infrared beam; for each glass chip 3–5 points (50 × 50 μm spot size) were analysed. Experimental glasses were double-polished to obtain 100–300 μm thin wafers, and then carefully washed under acetone and ethanol in order to remove any impurities. The areas of the sample analysed were always checked optically to avoid bubble or impurities. The thickness of each glass chip was measured microscopically during the analysis, with an uncertainty of ±1–3 μm. Absorption spectra were converted in H₂O concentration according to the Beer–Lambert equation:

$$C \text{ (wt\%)} = (MW * A) / t * \rho * \epsilon, \quad (1)$$

where C (wt%) is the water content dissolved in the melt, MW the molecular weight of water, A the height of the absorbance peak, t the thickness (cm) of the glass wafer, ρ the density (g/l) of the glass and ε the molar absorption extinction coefficient (L·mol⁻¹·cm⁻¹). To calculate the water content, we considered the absorption bands at 5200 cm⁻¹ (molecular H₂O) and 4500 cm⁻¹ (OH⁻ concentration) of the IR spectra. Only for a few samples the fundamental OH⁻ stretching vibration at 3530 cm⁻¹ was also measured, which required glass wafers of extremely thin thickness (<30 μm); thickness measures in the range 40–60 ± 2 μm are affected by a relative error of 2–5% while for a higher range of

Table 3. Experimental conditions and results of near-infrared FT-IR spectroscopy, elemental analyser and KFT analyses

	<i>T</i> (°C)	<i>P</i> (MPa)	H ₂ O _t (wt%- EA)	H ₂ O (wt%- KFT)	Density (g/L)*	Density (g/L)**	Thickness (cm)	A (OH ⁻)	sd	A (H ₂ O _{mol})	sd	OH (wt%)	sd	H ₂ O _m (wt%)	sd	H ₂ O wt% (FT-IR)	sd
Trachyte Starting Material					2330	2590											
GTT R11-1	950	50	2.86		2317		0.0273	0.0433	0.0039	0.0768	0.0060	1.35	0.03	1.33	0.10	2.68	0.07
GTT R10-1	950	100	3.84		2310	2460	0.0268	0.0525	0.0037	0.1210	0.0041	1.81	0.14	2.19	0.14	4.00	0.26
GTT R 9-1	950	150	4.95		2308		0.0177	0.0380	0.0016	0.1062	0.0044	1.92	0.04	2.86	0.11	4.78	0.13
GTT R 15-1	985	200	5.98 (±0.08)		2304		0.0193	0.0410	0.0023	0.1514	0.0094	1.89	0.20	3.70	0.24	5.73	0.42
GTT R 18-2	985	200	5.87 (±0.23)		2304		0.0208	0.0424	0.0032	0.1780	0.0102	1.81	0.15	4.03	0.29	5.89	0.28
GTT R16-1	985	300	6.87 (±0.04)		2298	2400	0.0286	0.0644	0.0062	0.3294	0.0083	2.00	0.19	5.42	0.11	7.42	0.25
GTT R19-1	985	300	7.37 (±0.20)		2400		0.0211	0.0415	0.0054	0.1980	0.0143	1.75	0.21	4.42	0.29	6.17	0.45
Pantellerite Starting Material (Pan113)					2471	2547											
Pan113 Run C-Run L	850	50	2.61	2.59	2411	2434	0.0178	0.0327	0.0015	0.0633	0.0015	1.14	0.13	1.41	0.13	2.56	0.26
Pan113 Run A-RunH	850	100	4.62 (±0.06)	4.53	2345	2390	0.0196	0.0460	0.0026	0.1528	0.0155	1.49	0.12	3.17	0.36	4.66	0.35
Pan113 Run B2	850	150	5.30 (±0.22)	5.22	233	2366											
Pan113 Run F-Run I	850	200		5.79	2382	2404	0.0182	0.0415	0.0031	0.1953	0.0033	1.43	0.11	4.29	0.10	5.72	0.20
Pan113 Run I	850	200			2310		0.0172	0.0375	0.0019	0.1813	0.0041	1.40	0.06	4.35	0.08	5.75	

Density (g/L)*: Density calculated from Archimedean density measure; Density (g/L)**: density from Ochs and Lange [1999] procedure; AOH- and A_{H₂O}: absorbance; sd: standard deviation.

thickness measures (~200 µm) an incertitude in ±10 correspond to a relative error of 5%.

4. Results

4.1. Microscopic observation and major element analyses

The run products consisted of microlite-free glasses. Most of the quenched glasses present also bubbles at the melt/capsule interface indicating fluid saturation during the experiment; however, bubble content never exceeded the 0.1 vol.%. Major element composition of experimental glasses (Table 1) resulting from analyses with a defocused beam (10 × 10 µm) [Morgan and London, 2005] matches in a high extent the composition of starting materials.

4.2. Water solubility in trachyte and pantelleritic melts

The total H₂O content dissolved in experimental glasses is reported in Table 3. Water content ranges from 2.9 wt% at 50 MPa to 7.1 wt% at 300 MPa for trachytic experimental glasses. At 200 and 300 MPa, two additional experiments were performed to check for the reproducibility of H₂O solubility at high pressure (Table 3). In pantelleritic experimental glasses,

the water content ranges from 2.6 at 50 MPa to 5.8 at 200 MPa and also in this case two additional experiments were performed at 2 MPa (Table 3). Figure 3(a,b) shows the variation of water content dissolved in the melt against pressure, confirming the general trend of increasing melt water content with increasing pressure as observed for all silicate melts (from basalt to rhyolite). The water solubility data in trachyte melt as a function of pressure can be described through an equation of the form $C_{H_2O_{melt}} = 0.3557 * P^{0.526}$ ($R^2 = 0.994$), where *P* is pressure in MPa. For pantellerites, a similar power law describes the variation of melt water content with pressure reading as: $C_{H_2O_{melt}} = 0.2786 * P^{0.5834}$ ($R^2 = 0.957$). All experimental studies on trachyte and pantellerite melts show an increase of melt water concentration with pressure but yield different slopes. Our experimental results will be compared below with available experimental data on Campi Flegrei trachytes [Di Matteo et al., 2004, Fanara et al., 2015] and with the experimental data of Stabile et al. [2018] on Kenyan haplo-pantellerites.

4.3. Analyses of IR spectra and molar absorption coefficients calibration

The bands of IR spectra at 5200 cm⁻¹ and 4500 cm⁻¹ for water species are the most used to determine water content in geological samples (Figure 4). The

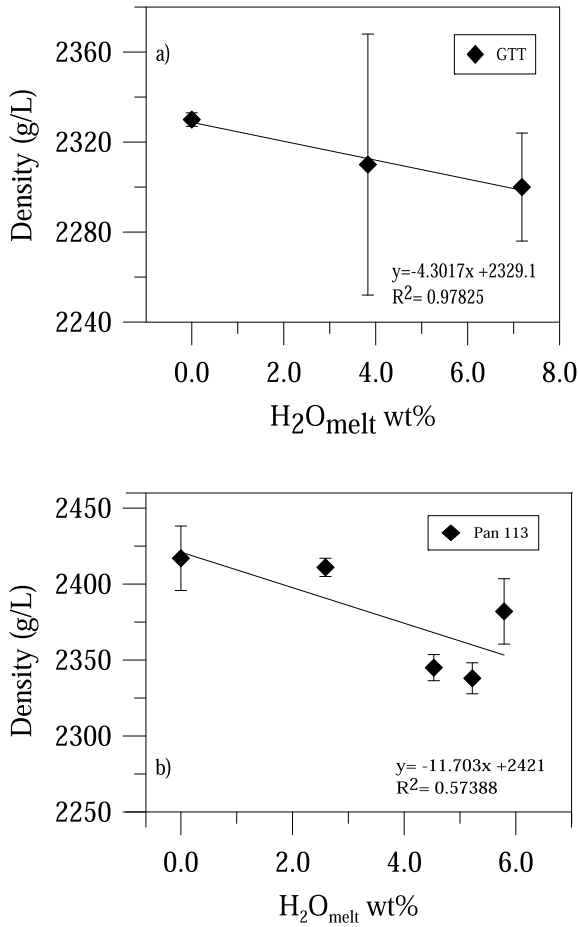


Figure 2. Dissolved H_2O_{melt} versus glass density measured through the Archimedeian method. Error bars indicate the standard deviation of repeated (~ 10) measures.

former is assigned to the combination of stretching and bending mode of H_2O molecules (H_2O_m) while the second to the combination of stretching and bending of hydroxyls (OH^-) groups [Stolper, 1982]. To avoid an incorrect estimation of absorption band peak height, a baseline correction is required. Following the previous studies of Withers and Behrens [1999], Ohlhorst *et al.* [2001] and Mandeville *et al.* [2002], we used a simple straight baseline [TT baseline, Ohlhorst *et al.*, 2001] connecting 4500 and 5200 backgrounds. We preferred to use this simple procedure knowing that a possible small underestimation of OH^- band cannot be excluded, owing to the presence of the 4000 cm^{-1} band. As suggested by Stabile *et al.* [2020], depending on sample compo-

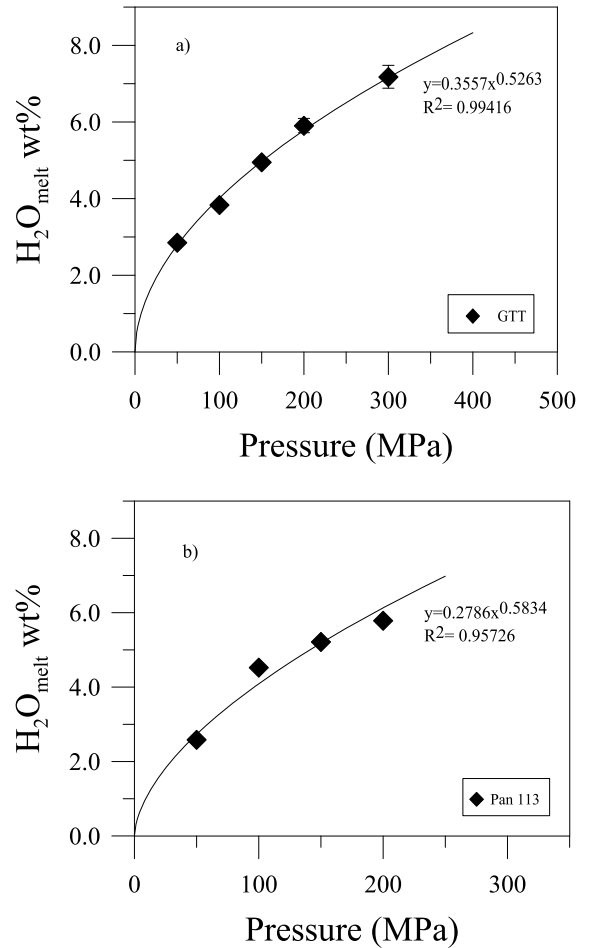


Figure 3. Dissolved H_2O_{melt} as a function of pressure for trachyte (a) and pantellerite (b) melt compositions.

sition and spectral variation, a critical evaluation of the approach used for the baseline correction has to be taken into account. Absorbance (peak intensity), density and thickness of the glass allow us to determine molar absorption coefficients (ϵ), in our case for the bands of molecular H_2O (5200 cm^{-1}) and OH^- groups (4500 cm^{-1}). The total water content dissolved in the experimental glasses is the sum of water species (H_2O_m and OH^-) and the Beer–Lambert equation can be rewritten as:

$$C\text{ (wt\%)} = C_{H_2O} + C_{OH^-} = 18.01 * A_{4500} / \rho * t * \epsilon_{4500} + 18.01 * A_{5200} / \rho * t * \epsilon_{5200}. \quad (2)$$

Knowing C (wt%) from KFT or EA, Equation (2) can be solved to determine the molar absorption

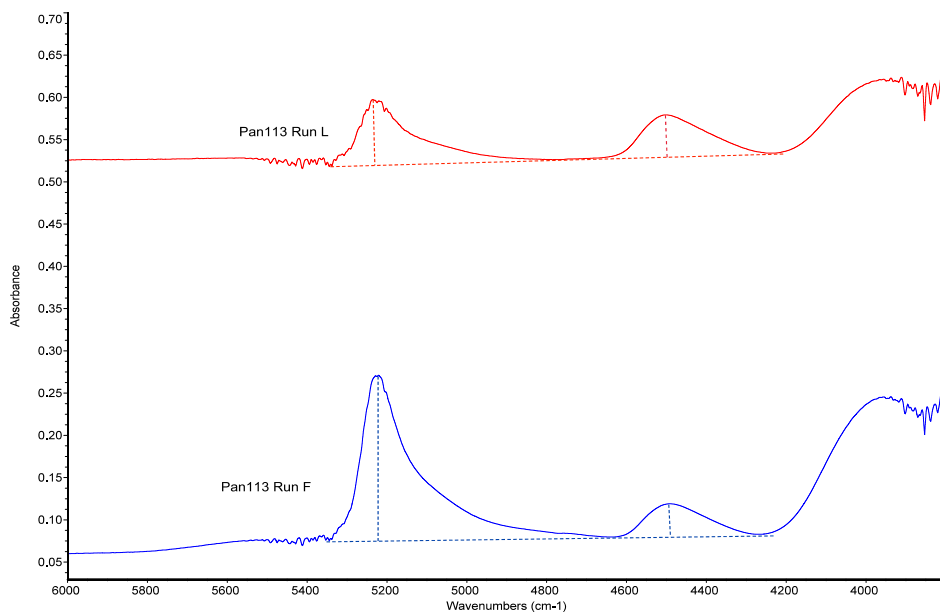


Figure 4. Near-infrared spectrum showing the two peaks related to OH^- group (at 4500 cm^{-1}) and molecular water (5200 cm^{-1}). The dashed lines tangential to the minima connecting the 4500 and the 5200 cm^{-1} peaks are illustrated to indicate the TT baseline correction procedure.

coefficients by plotting the absorbance of 5200 and 4500 bands normalized to density, thickness and water content. Using a linear regression the intercepts on X and Y axes are the ϵ_{4500} and ϵ_{5200} values (Figure 5a,b). Molar absorption coefficients were calculated assuming a linear relationship between the water species concentration and intensities of IR spectra bands. We obtained, for trachytic glasses, absorption coefficients of $0.88\text{ L/mol}\cdot\text{cm}^{-1}$ (ϵ_{4500}) and $1.6\text{ L/mol}\cdot\text{cm}^{-1}$ (ϵ_{5200}) while for pantellerite glasses ϵ_{4500} is $1.21\text{ L/mol}\cdot\text{cm}^{-1}$ and (ϵ_{5200}) $1.89\text{ L/mol}\cdot\text{cm}^{-1}$. Molar absorption coefficients are calibrated for a melt water content ranging between 2.6 and 7.4 in trachytic glasses and between 2.6 and 5.8 for pantelleritic ones. Regarding the uncertainties on the thickness and density measures, we can consider that the epsilon values are affected by relative errors in the range 2 – 7% .

5. Discussion

5.1. Comparison with previous works

(i) Trachyte compositions. Di Matteo *et al.* [2004] and Fanara *et al.* [2015] presented solubility experi-

ments on Campi Flegrei trachytes, obtained between 25 and 50 MPa (Figure 6a,b). Campi Flegrei trachytes are broadly similar in composition to Pantelleria trachytes, having a lower content in calcium, aluminium, potassium together with similar or slightly higher contents in silica, iron and sodium. Our solubility curve differs significantly from that of Di Matteo *et al.* [2004]. For instance, at 100 MPa the GTT melt has $\sim 1.2\text{ wt}\%$ less H_2O compared to the trend obtained by Di Matteo *et al.* [2004], the difference between the two sets of data increasing with pressure. Considering also the more mafic trachyte used by Di Matteo *et al.* [2004] (Pr38P), the difference in water content at 150 and 200 MPa is 0.94 to $1.6\text{ wt}\%$ lower. Compared to the experimental results of Fanara *et al.* [2015], melt water contents in our experiments are $0.4\text{ wt}\%$ to $0.7\text{ wt}\%$ higher in the investigated pressure range (100 – 300 MPa). The relationship between water solubility and pressure can be also compared with the calculated water solubility models of Moore *et al.* [1998], Papale *et al.* [2006] and Ghiorso and Gualda [2015] using GTT and Pan113 as starting compositions. Calculated values with Papale *et al.* model are higher by $0.5\text{ wt}\%$ to $1\text{ wt}\%$, depending on pressure, while Ghiorso and Gualda [2015]’s model calculates

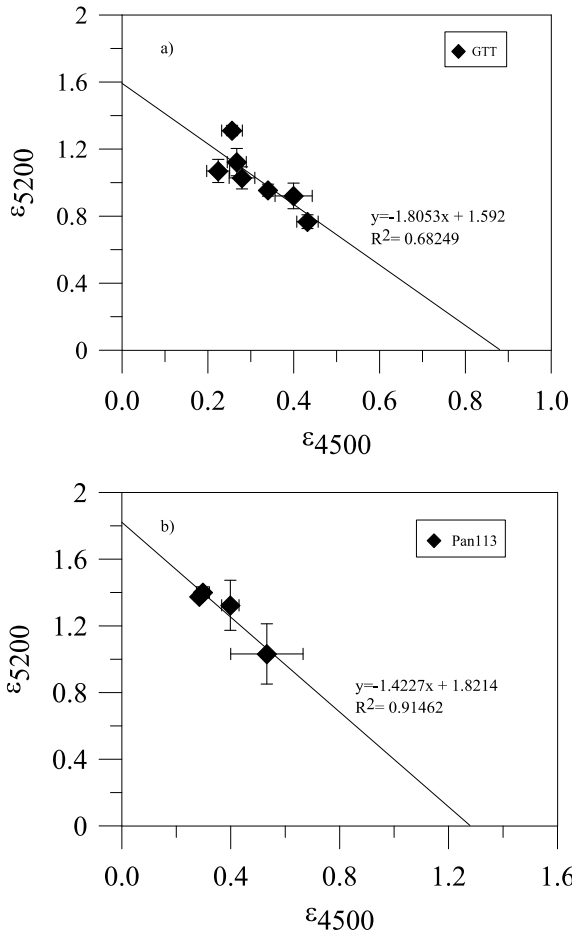


Figure 5. Resolution of Equation (2) in the text to obtain the molar absorptivity coefficient ϵ_{4500} and ϵ_{5200} . Each point is calculated from Equation (2). Normalized absorbance obtained for (a) trachyte and (b) pantellerite.

values that are higher by 0.3–0.7 wt% below 200 MPa, but at pressures >300 MPa the difference exceeds 1 wt%. On the contrary, Moore *et al.* [1998] matches better our experimental data, to within 0.1–0.4 wt% (Figure 6a).

(ii) Pantellerite compositions. Our experimental results on pantelleritic melt can be compared with the recent experimental works of Stabile *et al.* [2018] and Moore *et al.* [1998]. The solubility curves show notable differences, the water content of our pantelleritic melt at 100 MPa being ~1 wt% lower and up to ~2 wt% lower at higher pressure relative to the data of Stabile *et al.* [2018]; our solubility data are very simi-

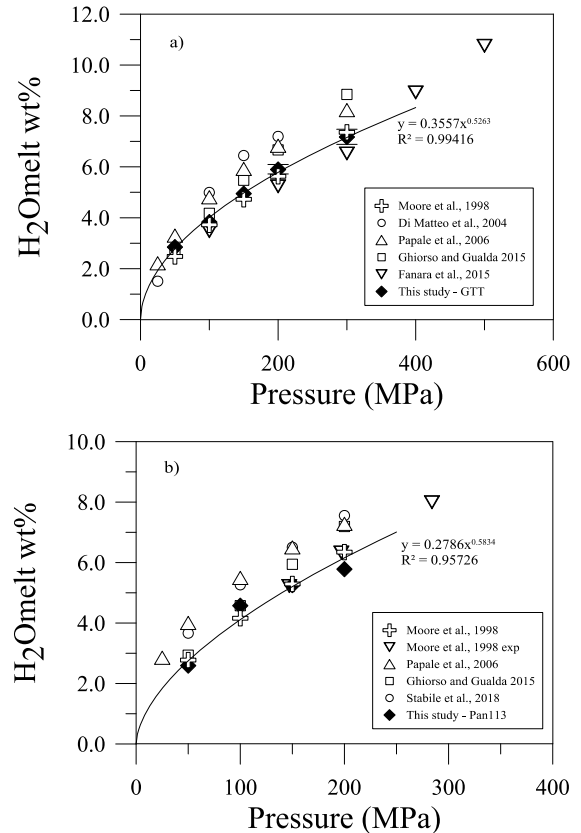


Figure 6. Water contents solubilized in the melt as a function of pressure obtained in this study for trachyte and pantellerite compared with (a) Di Matteo *et al.* [2004], Fanara *et al.* [2015] experimental data and solubility models of Moore *et al.* [1998], Papale *et al.* [2006] and Ghiorso and Gualda [2015]. Experimental results on pantellerite compared with (b) Moore *et al.* [1998], Stabile *et al.* [2018] experimental data and solubility models of Moore *et al.* [1998], Papale *et al.* [2006] and Ghiorso and Gualda [2015].

lar to the experimental results of Moore *et al.* [1998] at 150 and 200 MPa (Figure 6b) remembering that Stabile *et al.* data are based on synthetic pantellerite. The water solubility model of Papale *et al.* [2006] predicts water content higher than 1 wt% to 1.5 wt% than those of our experiments while considering the Ghiorso and Gualda [2015]'s model, the difference between the calculated solubility and the experimental data ranges between 0.2 wt% and 1.2 wt%. Over-

Table 4. Chemical composition of trachyte [Di Matteo *et al.*, 2004] and pantellerite [Moore *et al.*, 1998, Stabile *et al.*, 2018] used in other experimental studies

	Di Matteo <i>et al.</i> [2004] ZAC	Fanara <i>et al.</i> [2015]	This study GTT	Moore <i>et al.</i> [1998] NZC-4	Stabile <i>et al.</i> [2018] Ebu-B	This study Pan 113
SiO ₂	61.71	60.31	64.12	71.8	76.58	69.45
TiO ₂	0.45	0.42	0.85	0.24		0.48
Al ₂ O ₃	18.56	18.32	15.04	9.7	8.48	10.15
FeO*	3.17	5.21	6.27	5.77	5.48	7.87
MnO	0.27		0.27	0.14		0.21
MgO	0.23	1.31	0.62	0.01	0.02	0.1
CaO	1.64	4.11	1.48	0.2	0.23	0.53
Na ₂ O	6.11	2.81	6.58	5.3	4.72	6.71
K ₂ O	7.09	7.47	4.6	4.47	3.68	4.46
P ₂ O ₅	0.02		0.17	0.02		0.04
Total	99.25	100.08	100	97.6	99.2	100
P.I.	0.95	0.69	1.05	1.40	1.39	1.40

all, the model of Moore *et al.* [1998] better reproduces our experimental solubility data, these latter resulting lower by 0.1 to 0.5 wt% of the calculated ones. In contrast, the model of Papale *et al.* [2006] tends to overestimate significantly the melt water contents of our compositions.

(iii) The effect of small variations in bulk composition. To a first approximation, these differences in water solubility can be ascribed to small differences in chemical composition between the starting materials considered (Table 4). As stated previously, the dependence of water solubility in trachyte and pantelleritic melts with respect to small variation in chemical composition has not yet been fully investigated. For instance, the trachyte of this study has aluminium and potassium content almost 3 wt% lower with respect to the trachyte and trachyphonolite of Di Matteo *et al.* [2004] and Fanara *et al.* [2015] which has a higher K/Na ratio (0.71 respect to 0.46 of GTT trachyte); on the contrary, the GTT trachyte has higher silica and iron contents. Considering pantelleritic composition [Moore *et al.*, 1998, Stabile *et al.*, 2018], the differences in water solubility are also related to slight differences in melt composition (Table 4). Our pantellerite and that of Moore *et al.* [1998] indeed present similar oxides concentration with respect to that of Stabile *et al.* [2018], which has lower iron, aluminium, sodium and higher silica content. Water solubility has been also shown to correlate positively with metal ionization potential and negatively with Al₂O₃ content [Behrens and Jantos, 2001, Mysen, 2002]. Di Matteo

et al. [2004] and Stabile *et al.* [2018] explored the effect of alkalis on water solubility evidencing that for both trachyte and pantellerite melts, higher Na content favour H₂O incorporation in the melt, in accord with other studies on silicic compositions [Holtz *et al.*, 1995, Dingwell *et al.*, 1997, Carroll and Blank, 1997]. All these effects may explain the range in water contents obtained at the same P–T between the different sets of experiments. We note, however, that our comparison with previous experimental studies does not take into account the difference in experimental temperature, yet a clear relationship between temperature and water solubility has been evidenced for rhyolite [Yamashita, 1999] and phonolite melts [Schmidt and Behrens, 2008]. Such an effect still needs to be determined for peralkaline felsic compositions.

5.2. Effect of molar absorption coefficients

The molar absorption coefficients determined for our experimental glasses differ from those determined previously for trachytic by Di Matteo *et al.* [2004] and Fanara *et al.* [2015] and pantelleritic glasses by Stabile *et al.* [2020]. As stated above, molar absorption coefficients are determined assuming that they are constant over the range of water contents considered [Silver *et al.*, 1990]. The general agreement between water contents obtained with EA (Figure 7a) and KFT (Figure 7b) versus the total water content obtained by FT-IR spectroscopy, using the calibrated absorption coefficients, supports such an

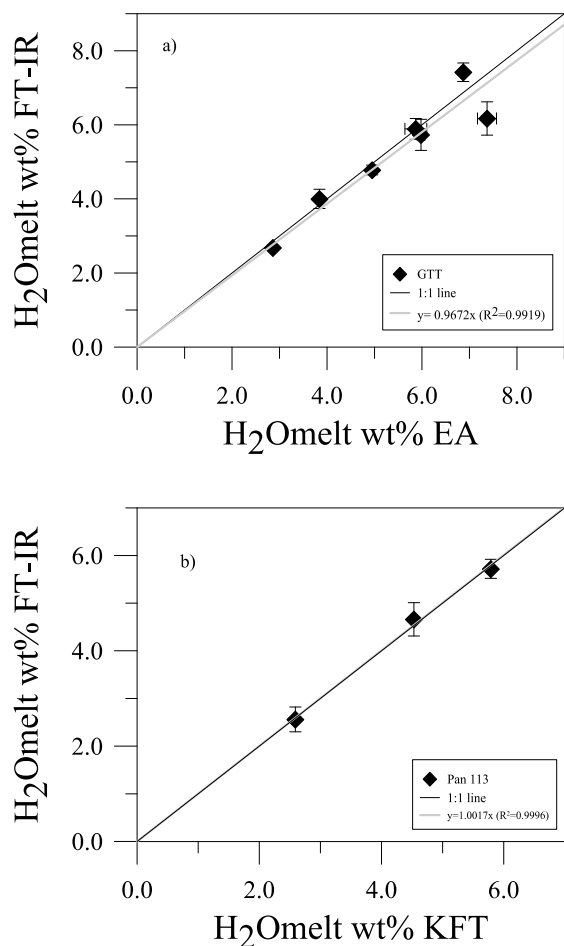


Figure 7. Total water content measured by elemental analyser (EA) and KFT versus water content obtained from FT-IR spectroscopy analysis for (a) trachyte and (b) pantellerite.

assumption (Figure 7a,b). There is a general consensus on the fact that absorption coefficients are composition dependent. Dixon *et al.* [1995] evidenced that absorption coefficients (ϵ_{4500} , ϵ_{5200}) correlate positively with the sum of cations Si and Al, suggesting that such a linear relationship can be used to calculate molar absorptivities of silicate melts. Other studies have shown a relation of ϵ with Na/K ratio, silica content and excess of aluminium [Stolper, 1982, Silver *et al.*, 1990, Behrens *et al.*, 1996] while Ohlhorst *et al.* [2001] reported a systematic increase of absorption coefficients from basalt to rhyolite and proposed a parabolic equation to calculate ϵ as a

function of silica content. The calculated absorption coefficients proposed for glasses having similar SiO₂ content to our trachyte and pantellerite [Ohlhorst *et al.*, 2001] are broadly similar to that determined in our study; yet, several authors [e.g. Dixon *et al.*, 1995, Mandeville *et al.*, 2002] suggest that a direct calibration for a specific composition yield to most accurate results. With respect to the published epsilon values on trachyte, we note that our epsilon values are 14–45% higher for ϵ (H₂O) and 26–44% lower for ϵ (OH); for pantelleritic glasses, ϵ (H₂O) is 2% lower and ϵ (OH) is 20% higher with respect to the value of Stabile *et al.* [2020]. Anyway, we used the absorption coefficients obtained in the studies on experimental glasses of Di Matteo *et al.* [2004], Fanara *et al.* [2015] for trachyte and Stabile *et al.* [2020] for pantellerite (Table 5). Using the absorption coefficients obtained by Di Matteo *et al.* [2004] to determine the water content from our IR spectra decreases the retrieved values; for instance, at 100 MPa the melt water content decrease from 5 to 4.6, i.e. values are 8% lower. On the other hand, if our absorption coefficients are used on the data of Di Matteo *et al.* [2004], their water contents increase by 0.1–0.6 wt%. Doing the same exercise on pantelleritic glasses, and using the absorption coefficients of Stabile *et al.* [2020], the water content increase by 0.04–0.4 wt%. Using our absorption coefficients for the data of Stabile *et al.* [2020], the water content decrease by 0.2–0.5 wt%. Differences in absorption coefficients influence above all the estimation of water species that could reflect either an incorrect estimation of OH⁻ relative to molecular species or the opposite. Taking as an example our results on pantellerite glasses, the OH/H₂O_m ratio increases from 0.07 to 0.2 when the absorption coefficients of Stabile *et al.* [2020] are used (i.e. ϵ_{4500} is 0.98 L/(mol·cm⁻¹) instead of 1.21 L/(mol·cm⁻¹) as determined in our study).

5.3. Water speciation

Water species concentration (OH⁻ and H₂O_m) in the experimental glasses as a function of total water content are shown in Figure 8a,b, for trachyte and pantelleritic glasses. As already shown for other quenched hydrous glasses, the OH⁻ group concentration is higher at low water content whereas molecular H₂O dominates for water contents above ~3 wt% [e.g. Stolper, 1982, Xue and Kanzaki, 2004, Dixon

Table 5. Molar absorption coefficients for OH⁻ and H₂O_m species for trachyte and pantellerite hydrous glasses

	SiO ₂ (wt%)	Al ₂ O ₃ (wt%)	Na/Na+K	ϵ (OH) L/mol·cm ⁻¹	ϵ (H ₂ O) L/mol·cm ⁻¹
Trachyte					
This Study	64.12	15.04	0.47	0.88	1.6
Di Matteo <i>et al.</i> [2004]	61.71	18.56	0.35	1.58	1.36
Fanara <i>et al.</i> [2015]	60.31	18.32	0.19	1.19	0.98
Pantellerite					
This Study	69.45	10.15	0.49	1.21	1.89
Stabile <i>et al.</i> [2020]	76.6	8.55	0.45	0.98	1.92

et al., 1995, Carroll and Blank, 1997, Withers and Behrens, 1999]. Our experimental glasses have water contents higher than 2.5 wt% so that we cannot appreciate the water speciation at low water concentrations. Anyway, it is evident in Figure 8a that the experimental glass with ~2.5 wt% represents the point at which OH⁻ and H₂O_m are present at equivalent concentrations. This appears less clear in the experimental glasses of pantelleritic composition, in which molecular water is slightly higher than OH⁻ at total water contents around 2.5 wt%. However, the speciation model of Dixon *et al.* [1995] and the experimental results on water speciation seem to be in good agreement within errors. Molecular water and hydroxyl species proportion in the experimental glasses at room temperature may reflect the structural re-equilibration during quench; this leads to an increase of molecular H₂O over hydroxyls with respect to the proportions at high temperature and pressure conditions [Silver *et al.*, 1990, Zhang *et al.*, 1995, Nowak and Behrens, 1995, Carroll and Blank, 1997]. For instance, Withers and Behrens [1999] investigated the effect of quenching on rhyolitic glasses containing 3 and 5 wt% H₂O. Glasses with initial OH/H₂O ratios of 1 and 0.6, after being reheated at 800 °C and at 300 MPa and rapidly quenched, showed a slight increase of their OH/H₂O ratios (1.17 and 0.72, respectively); they inferred that effect of quenching rate on water speciation was relatively minor at that melt water content. This gives information on the apparent equilibrium temperature (T_{ae}) [Zhang, 1994, 1999] considered the equilibrium temperature corresponding to the final speciation. However, we do not have sufficient data to appreciate if such a conclusion equally applies to other melt water contents.

5.4. Volcanological implications

Trachyte and pantellerite of Pantelleria show a similar capability to solubilize water content in the melt. We note only a subtle difference between the two compositions, water content in pantellerites being slightly higher (but always <1 wt%) with respect to trachytes. As evidenced by several works performed on melt inclusions [Lanzo *et al.*, 2013, and references therein], water contents characteristic of natural pantellerites of Pantelleria are in the range 2–4.9 wt%. To date, the difference in H₂O content has not yet been related with changes in eruptive dynamic of pantelleritic products (lava flow, strombolian and sub-plinian eruptions). However, a part of water, other factors can play an important role in controlling the eruptive styles [Cassidy *et al.*, 2018] as already identified for mafic volcanism in a typical basaltic volcano as Mt. Etna [Moretti *et al.*, 2018, and reference therein]. The study of water solubility in silicate melts has several implications for the study of hydrous natural glasses (melt inclusions and glass matrices). Ideally, melt inclusion studies allow one to assess the pre-eruptive volatile content of a magma, which can be then used to infer the (minimum) entrapment pressure (i.e. storage conditions if entrapment occurs in the reservoir) considering adequate solubility models and absence of diffusion towards the host crystal, post entrapment crystallization, etc. In the case of Pantelleria, several recent studies have determined the volatile content of melt inclusions trapped in phenocrysts of trachytic and pantelleritic rocks [Neave *et al.*, 2012, Lanzo *et al.*, 2013, Romano *et al.*, 2019] of some key explosive eruptions. The maximum water content measured in melt inclusion with pantelleritic composition was

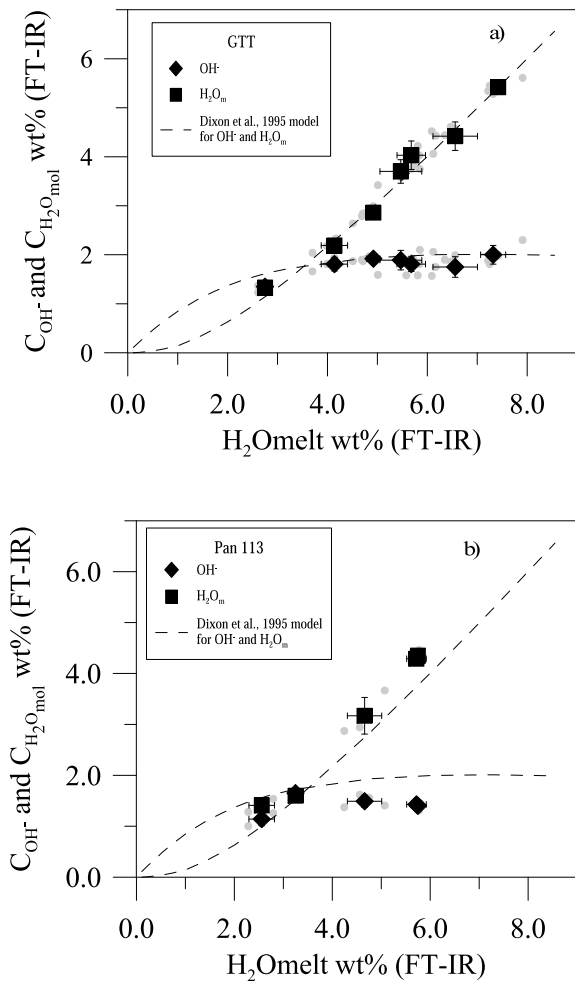


Figure 8. Water speciation in experimental glasses in (a) trachytic and (b) pantelleritic compositions. Grey dots are single point analysis while black ones represent the average values. Experimental data are compared with the model of Dixon et al. [1995].

4.5 wt% [Lanzo et al., 2013] while the water content estimated for trachytic melt through thermodynamical modelling and mass balance by White et al. [2009] ranges between 3.4 and 4 wt%. Romano et al. [2019] report water contents in melt inclusions of trachytic composition (0.15 to 1.05 wt%), suggesting that melt inclusions experienced volatile loss through the crystals. Considering 4 wt% of water dissolved in the trachytic melt, the protracted crystallization to generate a pantellerite liquid derivative [~80% of crystallization;

White et al., 2009, Romano et al., 2018] will lead to an excess of volatiles in the magmatic system and a consequent outgassing of volatiles, which could be the deep source of the diffusive degassing observed at Pantelleria nowadays.

Considering now the results of phase equilibria obtained on representative trachyte and pantellerite magmas, the magmatic felsic system of Pantelleria is inferred to evolve close to water saturation conditions, water and chlorine (during the late stage of evolution) being the dominant volatile species [Lanzo et al., 2013]. Evolution at volatile saturation conditions has been recently proposed for similar peralkaline magmatic systems elsewhere [Iddon and Edmonds, 2020] with reservoirs located at pressures <200 MPa. Using the highest water content measured in trachytic and pantelleritic melt inclusions at Pantelleria (water is the main volatile component, with no detectable CO₂), the model of Papale et al. [2006] gives storage pressures between 55 and 75 MPa for trachyte and pantellerite, respectively. Our experimental data constrain a pressure range between 70 and 110 MPa, or values which are 30% higher. Evolution of peralkaline felsic magmas in shallow reservoirs around 100 MPa is suggested by phase equilibrium and geophysical constraints [e.g. Di Carlo et al., 2010, Mattia et al., 2007]. Although such a difference might appear small, it corresponds to a difference of the top-depth of magma storage region (calculated assuming an average crustal density of 2600 kg·m⁻³) of ~1 km. Underestimating by ~1 km the depth of magma storage region in a shallow volcanic system such as Pantelleria might have important consequences with regard to volcanic hazard issues; for instance, it will affect the estimated travel time needed for the magma to breach the surface. The difference in solubilities may also affect the magma porosity evolution during magma ascent as simulated in numerical models, with an obvious impact on the explosive–effusive transition: the critical porosity of 70% beyond which fragmentation of an ascending magma might occur, will happen at deeper levels in a model using our solubility data instead of that of Di Matteo et al. [2004]. This underscores the importance of using accurate volatile solubility laws, hence the need to carry out specific hydrothermal experiments on representative compositions, if those laws are not available or if models are used too far from the compositional calibrated range.

6. Conclusions

This study was aimed at constraining the water solubility in trachyte and pantellerite melts from Pantelleria island. It is largely accepted that the solubility of water in silicate melt is composition-specific not only at the broad scale (silica-rich, silica-poor magmas) but also for variations in major element abundance within the same magma type (for instance, Pantelleria trachyte and Campi Flegrei trachyte). We thus performed this experimental study in order to add to the existing experimental data set on water solubility in felsic magmas, the missing data for trachytes straddling the chemical divide that separates metaluminous from peralkaline magmas. Our results place tighter constraints on water solubility-related arguments specific to eruptive phenomena (eruption style, pre-eruptive conditions, magmatic outgassing) but also on fundamental petrogenetic processes in which dissolved water plays a role (i.e. liquid line of descent oriented towards pantellerite melts).

Experiments were carried out in a pressure range 50–300 MPa in an IHPV, with only H₂O as the sole volatile component. The FT-IR study of experimental glasses resulted in the definition of the following molar absorptivity coefficients $\epsilon_{4500} = 0.88 \text{ L/mol}\cdot\text{cm}^{-1}$ and $\epsilon_{5200} = 1.6 \text{ L/mol}\cdot\text{cm}^{-1}$ for trachyte and $\epsilon_{4500} = 1.21 \text{ L/mol}\cdot\text{cm}^{-1}$ and $\epsilon_{5200} = 1.89 \text{ L/mol}\cdot\text{cm}^{-1}$ for pantellerite glasses. Absorption coefficients are different from those estimated in other trachyte [Di Matteo *et al.*, 2004, Fanara *et al.*, 2015] or phonolite [Carroll and Blank, 1997] melt compositions, and hence contribute to define an important composition-specific variable needed for FT-IR studies of such melt compositions.

Our experimental data were tested against the models of Moore *et al.* [1998], Papale *et al.* [2006] and Ghiorso and Gualda [2015]. The Papale *et al.* [2006] model overestimates the H₂O_{melt} content for Na-rich magma, such as Pantelleria felsic magmas. This effect has significant implications when applied to the study of melt inclusions, whose volatile abundances are used to derive the depth of magma storage region. In the specific case of Pantelleria, trachyte and pantellerite storage pressure derived from the model of Papale *et al.* [2006] are about 50–70 MPa, for a dissolved H₂O content in the range 3.4–4.5 wt%, which implies a magma storage depth of ~2.4 km. Using our experimental solubility model the calculated depth

increases to ~3.5 km, a 30% difference, not trivial for such shallow magma bodies.

Acknowledgements

PR is deeply grateful for all the support received from the “MagmaTeam” of ISTO during the experimental work. IDC and JA acknowledge support from both LabEx VOLTAIRE (LABX-100-01) and EquipEx PLANEX (ANR-11-EQPX-0036) projects. The authors thank Paola Stabile and Michael R. Carroll for their thorough and helpful comments.

References

- Arzilli, F., Stabile, P., Fabbrizio, A., Landi, P., Scaillet, B., Paris, E., and Carroll, M. R. (2020). Crystallization kinetics of alkali feldspar in peralkaline rhyolitic melts: implications for Pantelleria volcano. *Front. Earth Sci.*, 8, article no. 177.
- Behrens, H. and Jantos, N. (2001). The effect of anhydrous composition on water solubility in granitic melts. *Am. Mineral.*, 86, 14–20.
- Behrens, H., Meyer, M., Holtz, F., Benne, D., and Nowak, M. (2001). The effect of alkali ionic radius, temperature and pressure on the solubility of water in MAISI3O8 melts (M = Li, Na, K, Rb). *Chem. Geol.*, 174, 275–289.
- Behrens, H., Misiti, V., Freda, C., Vetere, F., Botcharnikov, R., and Scarlato, P. (2009). Solubility of H₂O and CO₂ in ultrapotassic melts at 1200 and 1250 °C and pressure from 50 to 500 MPa. *Am. Mineral.*, 94, 105–120.
- Behrens, H., Ohlhorst, S., Holtz, F., and Champenois, M. (2004). CO₂ solubility in dacitic melts equilibrated with H₂O–CO₂ fluids: implications for modeling the solubility of CO₂ in silicic melts. *Geochim. Cosmochim. Acta*, 68, 4687–4703.
- Behrens, H., Romano, C., Nowak, M., Holtz, F., and Dingwell, D. B. (1996). Near-infrared spectroscopic determination of water species in glasses of the system MAISI3O8 (M = Li, Na, K): an interlaboratory study. *Chem. Geol.*, 128, 41–63.
- Botcharnikov, R. E., Behrens, H., and Holtz, F. (2006). Solubility and speciation of C–O–H fluids in andesitic melt at T = 1100–1300 °C and P = 200 and 500 MPa. *Chem. Geol.*, 229, 125–143.

- Carroll, M. R. and Blank, J. G. (1997). The solubility of H₂O in phonolitic melts. *Am. Mineral.*, 82, 1111–1115.
- Cashman, K. V. and Mangan, M. T. (1994). Physical aspects of magmatic degassing II: Constraints on vesiculation processes from textural studies of eruptive products. In Carroll, M., editor, *Volatiles in Magmas*, pages 447–478. Mineralogical Society of America.
- Cassidy, M., Manga, M., Cashman, K., and Bachmann, O. (2018). Controls on explosive-effusive volcanic eruption styles. *Nat. Commun.*, 9, article no. 2839.
- Di Carlo, I., Rotolo, S. G., Scaillet, B., Buccheri, V., and Pichavant, M. (2010). Phase equilibrium constraints on pre-eruptive conditions of recent felsic explosive volcanism at Pantelleria Island, Italy. *J. Petrol.*, 51, 2245–2276.
- Di Matteo, V., Carroll, M. R., Behrens, H., Vetere, F., and Brooker, R. A. (2004). Water solubility in trachytic melts. *Chem. Geol.*, 213, 189–196.
- Dingwell, D. B., Holtz, F., and Behrens, H. (1997). The solubility of H₂O in peralkaline and peraluminous melts. *Am. Mineral.*, 82, 434–437.
- Dingwell, D. B., Romano, C., and Hess, K. U. (1996). The effect of water on the viscosity of haplogranitic melt under P–T–X conditions relevant to silicic volcanism. *Contrib. Mineral. Petrol.*, 124, 19–28.
- Dixon, T. E., Stolper, E., and Holloway, J. R. (1995). An experimental study of water and carbon dioxide solubilities in mid-ocean basalt liquids: Part I. Calibration and solubility models. *J. Petrol.*, 36, 1607–1631.
- Fanara, S., Botcharnikov, R. E., Palladino, D. M., Adams, F., Buddensieck, J., Mulch, A., and Behrens, H. (2015). Volatiles in magmas related to the Campanian Ignimbrite eruption: Experiments vs. natural findings. *Am. Mineral.*, 100, 2284–2297.
- Ghiorso, M. S. and Gualda, G. A. R. (2015). An H₂O–CO₂ mixed fluid saturation model compatible with rhyolite-Melts. *Contrib. Mineral. Petrol.*, 169, article no. 53.
- Hamilton, D. L., Burnham, C. W., and Osborn, E. F. (1964). The solubility of water and effects on fugacity and water content on crystallization in mafic magmas. *J. Petrol.*, 5, 21–39.
- Holtz, F., Behrens, H., Dingwell, D. B., and Johannes, W. (1995). H₂O solubility in haplogranitic melts: compositional, pressure and temperature dependence. *Am. Mineral.*, 80, 94–108.
- Holtz, F., Behrens, H., Dingwell, D. B., and Taylor, R. P. (1992). Water solubility in aluminosilicate melts of haplogranite composition at 2 Kbar. *Chem. Geol.*, 96, 289–302.
- Holtz, F., Roux, J., Behrens, H., and Pichavant, M. (2000). Water solubility in silica and quartzofeldspathic melts. *Am. Mineral.*, 85, 682–686.
- Housh, T. B. and Luhr, J. F. (1991). Plagioclase-melt equilibria in hydrous systems. *Am. Mineral.*, 76, 477–492.
- Iacono-Marziano, G., Schmidt, B. C., and Dolfi, D. (2007). Equilibrium and disequilibrium degassing of a phonolitic melt (Vesuvius A.D. 79 “White Pumice”) simulated by decompression experiments. *J. Volcanol. Geoth. Res.*, 161, 151–164.
- Iddon, F. and Edmonds, M. (2020). Volatile-rich magmas distributed through the upper crust in the main Ethiopian rift. *Geochem. Geophys. Geosyst.*, 21.
- Johannes, W. and Holtz, F. (1996). Petrogenesis and experimental petrology of granitic rocks. In *Minerals and Rocks*, volume 22. Springer Verlag, Berlin. 335 pp.
- Lanzo, G., Landi, P., and Rotolo, S. G. (2013). Volatiles in pantellerite magmas: A case study of the Green Tuff Plinian eruption (Island of Pantelleria, Italy). *J. Volcanol. Geoth. Res.*, 262, 153–163.
- Larsen, J. F. and Gardner, J. E. (2004). Experimental study of water degassing from phonolite melts: implications for volatile oversaturation during magmatic ascent. *J. Volcanol. Geoth. Res.*, 134, 109–124.
- Lesne, P., Scaillet, B., Pichavant, M., Iacono-Marziano, G., and Beny, J. M. (2010). The H₂O solubility of alkali basalts: an experimental study. *Contrib. Mineral. Petrol.*, 162, 133–151.
- Liu, Y., Zhang, Y., and Behrens, H. (2005). Solubility of H₂O in rhyolitic melts at low pressures and a new empirical model for mixed H₂O–CO₂ solubility in rhyolitic melts. *J. Volcanol. Geoth. Res.*, 143, 219–235.
- Macdonald, R. (1974). Nomenclature and petrochemistry of the peralkaline oversaturated extrusive rocks. *Bull. Volcanol.*, 38, 498–505.
- Mandeville, C. W., Webster, J. D., Rutherford, M. J.,

- Taylor, B. E., Timbal, A., and Faure, K. (2002). Determination of molar absorptivities for infrared absorption bands of H₂O in andesitic glasses. *Am. Mineral.*, 87, 813–821.
- Mattia, M., Bonaccorso, A., and Guglielmino, F. (2007). Ground deformations in the island of Pantelleria (Italy): insights into the dynamic of the current intereruptive period. *J. Geophys. Res.*, 112, article no. B11406.
- Moore, G., Vennemann, T., and Carmichael, I. S. E. (1998). An empirical model for the solubility of H₂O in magmas to 3 kilobars. *Am. Mineral.*, 83, 36–42.
- Moretti, R., Metrich, N., Arienzo, I., Di Renzo, V., Aiuppa, A., and Allard, P. (2018). Degassing vs. eruptive styles at Mt Etna volcano (Sicily, Italy). Part I: Volatile stocking, gas fluxing, and the shift from low-energy to highly explosive basaltic eruptions. *Chem. Geol.*, 482, 1–17.
- Morgan, G. B. and London, D. (2005). Effect of current density on the electron microprobe analysis of alkali aluminosilicate glasses. *Am. Mineral.*, 90, 1131–1138.
- Moussallam, Y., Morizet, Y., Massuyeau, M., Laumonier, M., and Gaillard, F. (2015). CO₂ solubility in kimberlite melts. *Chem. Geol.*, 418, 198–205.
- Mysen, B. O. (2002). Water in peralkaline aluminosilicate melts to 2 GPa and 1400 °C. *Geochim. Cosmochim. Acta*, 66, 2915–2918.
- Neave, D. A., Fabbro, G., Herd, R. A., Petrone, C. M., and Edmonds, M. (2012). Melting, differentiation and degassing at the Pantelleria volcano, Italy. *J. Petrol.*, 53, 637–663.
- Nowak, M. and Behrens, H. (1995). The speciation of water in haplogranitic glasses and melts determined by in situ near-infrared spectroscopy. *Geochim. Cosmochim. Acta*, 59, 504–511.
- Ochs, F. A. and Lange, R. A. (1999). The density of hydrous magmatic liquids. *Science*, 283, 1314–1317.
- Ohlhorst, S., Behrens, H., and Holtz, F. (2001). Compositional dependence of molar absorptivities of near-infrared OH- and H₂O bands in rhyolitic to basaltic glasses. *Chem. Geol.*, 174, 5–20.
- Papale, P., Moretti, R., and Barbato, D. (2006). The compositional dependence of the saturation surface of H₂O + CO₂ fluids in silicate melts. *Chem. Geol.*, 229, 78–95.
- Richet, P., Lejeune, A. M., Holtz, F., and Roux, J. (1996). Water and the viscosity of andesite melts. *Chem. Geol.*, 128, 185–197.
- Romano, C., Dingwell, D. B., Behrens, H., and Dolfi, D. (1996). Compositional dependence of H₂O solubility along the joins NaAlSi₃O₈–KAlSi₃O₈, NaAlSi₃O₈–LiAlSi₃O₈, and KAlSi₃O₈–LiAlSi₃O₈. *Am. Mineral.*, 81, 452–461.
- Romano, P., Andújar, J., Scaillet, B., Romengo, N., Di Carlo, I., and Rotolo, S. G. (2018). Phase equilibria of Pantelleria trachytes (Italy): Constraints on pre-eruptive conditions and on the metaluminous to peralkaline transition in silicic magmas. *J. Petrol.*, 59, 559–588.
- Romano, P., Scaillet, B., White, J. C., Andujar, J., Di Carlo, I., and Rotolo, S. G. (2020). Experimental and thermodynamic constraints on mineral equilibrium in pantelleritic magmas. *Lithos*, 376–377, 1–22.
- Romano, P., White, J. C., Ciulla, A., Di Carlo, I., D’Orlando, C., Landi, P., and Rotolo, S. G. (2019). Volatiles and trace elements content in melt inclusions from the zoned Green Tuff ignimbrite (Pantelleria, Sicily): petrological inferences. *Ann. Geophys.*, 62(1).
- Scaillet, B. and Macdonald, R. (2006). Experimental constraints on pre-eruption conditions of pantelleritic magmas: evidence from the Eburru complex, Kenya Rift. *Lithos*, 91, 95–108.
- Scaillet, B., Pichavant, M., and Roux, J. (1995). Experimental crystallization of leucogranite magmas. *J. Petrol.*, 36, 635–705.
- Scaillet, B., Pichavant, M., Roux, J., Humbert, G., and Lefèvre, A. (1992). Improvements of the Shaw membrane technique for measurement and control of fH₂ at high temperatures and pressures. *Am. Mineral.*, 77, 647–655.
- Schmidt, B. C. and Behrens, H. (2008). Water solubility in phonolite melts: Influence of melt composition and temperature. *Chem. Geol.*, 256, 258–267.
- Silver, L. A., Ihinger, P. D., and Stolper, E. (1990). The influence of bulk composition on the speciation of water in silicate glasses. *Contrib. Mineral. Petrol.*, 104, 142–162.
- Sisson, T. W. and Grove, T. L. (1993). Experimental investigation of the role of H₂O in calcalkaline differentiation and subduction zone magmatism. *Con-*

- trib. Mineral. Petrol.*, 113, 143–166.
- Stabile, P., Appiah, E., Bello, M., Giuli, G., Paris, E., and Carrol, M. R. (2020). New IR spectroscopic data for determination of water abundances in hydrous pantelleritic glasses. *Am. Mineral.*, 105, 1060–1068.
- Stabile, P., Radica, F., Bello, M., Behrens, H., Carroll, M. R., Paris, E., and Giuli, G. (2018). H₂O solubility in pantelleritic melts: Pressure and alkali effects. *Neues Jahrbuch für Mineralogie—Abhandlungen*, 195, 1–9.
- Stolper, E. (1982). The speciation of water in silicate melts. *Geochim. Cosmochim. Acta*, 46, 2609–2620.
- Tamic, N., Behrens, H., and Holtz, F. (2001). The solubility of H₂O and CO₂ in rhyolitic melts in equilibrium with a mixed CO₂–H₂O fluid phase. *Chem. Geol.*, 174, 333–347.
- Watson, E. B. (1994). Diffusion in volatile-bearing magmas. In Carroll, M. R. and Holloway, J. R., editors, *Volatiles in Magmas*, volume 30 of *Review in Mineralogy*, pages 371–411. Mineralogical Society of America.
- White, J. C., Parker, D. F., and Ren, M. (2009). The origin of trachyte and pantellerite from Pantelleria, Italy: insights from major element, trace element, and thermodynamic modelling. *J. Volcanol. Geoth. Res.*, 179, 33–55.
- Withers, A. C. and Behrens, H. (1999). Temperature induced changes in the NIR spectra of hydrous albitic and rhyolitic glasses between 300 and 100 K. *Phys. Chem. Minerals*, 27, 119–132.
- Xue, Y. and Kanzaki, M. (2004). Dissolution mechanism of water in depolymerised silicate melts: constraints from H and Si NMR spectroscopy and ab initio calculations. *Geochim. Cosmochim. Acta*, 68, 5027–5058.
- Yamashita, S. (1999). Experimental study of the effect of temperature on water solubility in natural rhyolite melt to 100 MPa. *J. Petrol.*, 40, 1497–1507.
- Zhang, Y. (1994). Reaction kinetics, geospeedometry, and relaxation theory. *Earth Planet. Sci. Lett.*, 122, 373–391.
- Zhang, Y. (1999). H₂O in rhyolitic glasses and melts: measurement, speciation, solubility, and diffusion. *Rev. Geophys.*, 37, 493–516.
- Zhang, Y., Stolper, E. M., and Ihinger, P. D. (1995). Kinetics of reaction H₂O + O = 2OH in rhyolitic glasses: Preliminary results. *Am. Mineral.*, 80, 593–612.